Journal of Materials Chemistry B

Accepted Manuscript

ROYAL SOCIETY OF CHEMISTRY

www.rsc.org/materialsB

Bioabsorbable Cellulose Composites Prepared by an Improved Mineral-binding Process for Bone Defect Repair

Yang Hu[a,b], Yongjun Zhu[a], Xin Zhou[a], Changshun Ruan[a], Haobo Pan[a], Jeffrey M. Catchmark*[b]

[a]Center for Human Tissues and Organs Degeneration, and Shenzhen Key Laboratory of Marine Biomedical Materials, Institute of Biomedicine and Biotechnology, Shenzhen Institutes of Advanced Technology, Chinese Academy of Sciences, Shenzhen 518055, China

[b]Department of Agricultural and Biological Engineering, and Center for Nanocellulosics, Pennsylvania State University, University Park 16802, Pennsylvania, USA

***Corresponding author:** Jeffrey M. Catchmark, jcatchmark@engr.psu.edu

Abstract:

Bioabsorbable bacterial cellulose composites were prepared separately by immersing bacterial cellulose (BC) in different simulated body fluids (SBF) followed by incorporating cellulase enzymes into BC. The biomineralization of BC in SBF has been intensively documented and generally involves a tedious preparation. This study revealed an improved approach to disperse hydroxyapatite (HA) nanopowder to a saturated concentration (1.0×) of SBF, which was able to enhance the total amount of calcium phosphates (CPs) bound to BC composites. Such a simplified approach could be used to replace oversaturated concentration (1.5×) of SBF to prepare BC/CPs composites and achieve equal or even better material properties.

The incorporation of cellulosic enzymes into BC/CPs composites verified the bioabsorption of BC where composites were able to achieve an *in-vitro* bulk biodegradation with a yield of 96% glucose released. Cell culture of mouse osteoblasts also demonstrated the good biocompatibility of the BC/CPs composites prepared by using the simplified approach. This enzyme-incorporating BC/CPs composites studied show promise as bioabsorbable carriers delivering CPs for bone defect repair.

Key words: Bacterial cellulose; Cellulase; Bioabsorbability; Block-by-block degradation; Bulk degradation.

1. Introduction

The bone matrix is the major part of bone, and it consists primarily of inorganic calcium phosphates (CPs, a general name of apatites consisting of different ratios of Ca/P compounds, such as hydroxyapatite and tricalcium phosphate) and organic collagen. The formation of bone requires the solidification of this matrix around entrapped cells.[1] Bone defects occur when a part of the bone matrix is lost due to trauma and diseases.[2] If the bone wound condition is beyond self-healing, extraneous tissues or materials are required to fill the defect area to induce osseous tissue regeneration.[3]

Bacterial cellulose (BC) is a biopolymeric hydrogel. It has been extensively studied and commercialized in the biomedical market for wound care.[4] BC is an excellent alternative to other biomaterials due to good biocompatibility, excellent fluid exchange capability, diverse physical

morphologies and biomimetic mechanical properties.[5,6] It also has a porous structure making it promising for bone repair.[7] A few researchers have performed studies on BC for cartilage and bone scaffold applications.[8-10] For example, biomimetic BC/hydroxyapatite (HA) composites were prepared *in situ* where HA nanopowder was added to bacterial culture medium prior to the onset of cellulose biosynthesis to entrap HA in the BC reticular hydrogel.[11] Another method to prepare BC/HA composites involves immersing already-formed BC hydrogels into oversaturated simulated body fluid (SBF) solutions (the ionic concentration is 1.5 times higher than saturated concentration) and then allowing apatite layers to form on the BC surface.[12-17] These BC composites have shown good biocompatibility for both osteoblast cells and bone marrow stromal cells making them useful for applications involving bone regeneration. It is known, however, that BC is unable to biodegrade in the body as there are no *in-vivo* responsive cellulosic enzymes. This disadvantage has confined the application of BC as an *in-vivo* biomaterial.

One study revealed that BC implanted into an animal model over twelve weeks would not produce adverse effects, and was able to integrate with the host tissue after four weeks.[18] However, chronic responses (> one year) inside the host tissue were not reported in this study to indicate the underlying risk for BC in a long-term implantation. Complete degradation of BC in the body should enable BC to be an ideal material as its exclusive monomer is glucose which can support cell growth. In addition, unlike other degradable polymers, the release of glucose does not lower the pH preserving the environment conducive to osteoblast cell proliferation.[19,20] To date, few efforts have been made to enable BC biodegradable in the body. Oxidized cellulose is a typical absorbable cellulose developed by Ethicon (Johnson & Johnson Medical, Somerville, NJ).[21,22] Most oxidized cellulose materials can degrade within 48 h to 1000 h upon different oxidation approaches,[23,24] but they can hardly achieve nearly 100% degradation in the body.

Studies have shown that such a biodegradation of oxidized cellulose in the body is highly associated with erosion caused by macrophage processing rather than a hydrolytic degradation.[25] Meanwhile, the biodegradation of chemically-modified cellulose usually presents a block-by-block degradation behavior instead of a bulk degradation behavior in the body, suggesting an underlying foreign body reaction due to some material debris and somehow a low glucose yield due to *in-vivo* mild environment.[26-28] In order to achieve complete biodegradation of BC in the body, we previously developed a BC composite incorporating cellulase enzymes which exhibited a bulk degradation behavior as well as a high glucose yield (97%) *in-vitro* over a period of seven days.[29,30] The *in-vivo* model study also demonstrated that BC incorporating cellulase enzymes achieved a nearly complete degradation within 4 weeks, and those enzymes failed to bring any perceptible side-effects.[31]

It was believed that materials capable of growing apatite layers in SBF are bioactive and the Ca/P ratio of grown apatite layers is similar to physiological ratio of bone Ca/P.[17] However, recent opinions have pointed out that such a material mineralization in SBF is recognized as a cellular process, indicating that SBF immersion has virtually no biological meaning.[32,33] In this study, a novel BC composite was developed by an improved mineral-binding process. Rather than considering the bioactive efficacy of CPs produced from SBF immersion, we aimed to increase the amount of CPs bound to BC while simplifying the tedious BC/CPs composite preparation. HA nanopowder was dispersed in saturated SBF (1.0×) instead of oversaturated SBF (1.5×) where the addition of extra HA nanopowder in saturated SBF was expected to expedite and further increase the deposition of CPs on BC as compared to oversaturated SBF without HA nanopowder. By loading the enzyme to BC/CPs composites, we expected that BC would act biodegradably as not only a carrier to deliver CPs to bone defect sites, but also as a temporary

substrate for cell growth. Electron microscopy analysis, Fourier Transform Infrared Spectroscopy, X-ray Diffraction, and *in-vitro* degradation experiments were used to determine the efficacy of CPs bound to BC and the biodegradability of BC/CPs composites. Cell viability study using mouse embryo preosteoblast cells (MC3T3-E1) was performed to evaluate the preliminary biocompatibility of BC/CPs composites.

2. Materials and methods

2.1 Materials

A BC hydrogel was prepared via a static culture using the cellulose producing bacterium *Gluconacetobacter xylinus* (ATCC 700178). Cellulosic enzyme from *Trichoderma reesei* ATCC 26921 (Sigma C8546) and hydroxyapatite nanopowder (Aldrich 677418) were purchased and directly used without further purification.

2.2 Preparation of bioabsorbable BC/CPs composites

Pristine BC were cultured in a pH 5.0 medium inoculated by *G. xylinus* (1%, v/v) buffered by 3 mol/L hydrochloric acid. The protocol consisting of the medium composition, cellulose biosynthesis and purification were similar to those used in our previous study.[34,35] After 3-5 mm thick cellulose pellicles were formed in the medium and purified in 0.1 mol/L sodium hydroxide at 80 °C for 30 min, pellicles were rinsed in deionized (DI) water until they were free of alkali, fragments, medium ingredients and bacterial cells. The purified pellicles were stored as pristine BC hydrogels at 4 °C in DI water.

To produce bioabsorbable BC/CPs composites incorporating cellulosic enzymes, three physiologically relevant solutions were first prepared. The PBS solution, used as an environmental solution during the in-vitro material degradation, consisted of KCl, KH_2PO_4, NaCl and Na_2HPO_4, dissolved in DI water and then buffered to pH 7.4 with 3 M HCl.[36,37] The preparation of SBF involved dissolving NaCl, $NaHCO_3$, KCl, $K_2HPO_4 \cdot 3H_2O$, $MgCl_2 \cdot 6H_2O$ and $CaCl_2$ into DI water and then being buffered to pH 7.4 at 37 °C with 50 mM trishydroxymethyl aminomethane and 45 mM HCl.[36-38] Different concentrations of SBF containing saturated SBF with dispersed 1.0 mg of HA nanopowder (1.0×, HASBF) and oversaturated SBF (1.5×, 1.5SBF) were separately prepared where the ionic concentrations of chemicals dissolved in oversaturated SBF is 1.5 times as saturated SBF. In the meantime, the enzyme solution was prepared in 10 mL of pH 5.0 citric acid-sodium citrate buffer in which 80 mg of cellulosic enzyme was dissolved.

Next, to prepare bioabsorbable BC/CPs composites, the purified and freeze-dried BC was cut into approximately 2.5 × 2.5 cm square pieces, and then immersed in 0.1 mol/L of $CaCl_2$ at 37 °C for 48 h. After rinsing with DI water, the BC pieces were immersed in the HASBF and 1.5SBF solutions in a slow-rotating mixer at 37 °C for 7 days and 14 days, respectively. Both HASBF and 1.5SBF were used to compare the efficacy of CPs bound to BC and they were exchanged every two days. After rinsindrog and freeze-drying samples, 0.6 mL of enzyme solution was added dropwise on the BC pieces and then balanced for approximately 15 min to allow the enzyme solution to be evenly distributed. Finally, samples were again freeze-dried to obtain bioabsorbable BC/CPs composites.

2.3 Material characterization of BC/CPs composites

BC samples including untreated BC, 1.5SBFBC and HASBFBC treated for 7 days and 14 days were examined first using the Scanning Electron Microscopy (SEM, FEI-NANOSEM450, USA). To prepare samples for SEM observation operating at 5 kV, freeze-dried samples were coated with gold by a vacuum sputter coater to improve the conductivity prior to observation.

Thermogravimetric analyses (TGA) of all BC samples were performed by the TGA Q500 (TA Instrument, USA). Thermograms of samples were recorded between 40 °C and 600 °C at a heating rate of 10 °C /min and a nitrogen flow of 20 mL/min. TA Universal Analysis 2000 (TA Instrument, USA) was used to calculate the percentage of weight loss, the first derivatives of the thermograms (DTG), and the decomposition temperatures.

Examination of Fourier Transform Infrared Spectroscopy (FTIR) spectra for all BC samples followed the protocol as described by Gu and Catchmark.[39] Freeze-dried BC samples were placed on the FTIR spectrometer assembled with ATR sensor (Nicole 8700, Thermo Fisher, USA) by a high pressure clamp. FTIR data were taken from 4000 to 650 cm^{-1}. OMNIC software (Thermo Electron Corporation) was used to correct and normalize the baseline of FTIR spectra.

The crystallinity of all BC samples was analyzed using the PANalytical X'Pert Pro MPD theta-theta Diffractiometer (Almelo, Netherlands) with CuKα radiation (λ = 0.15406) generated at 40kV and 44 mA. To prepare BC samples for X-ray diffraction (XRD), the freeze-dried BC samples were first pressed by T-Rex system (TRX-1000-D) to obtain a nearly identical thickness. The compression was performed at 500 psi for 2 min, and the resulting samples then were cut to uniform sheets in a size of 2.5×2.5 cm. The XRD patterns of samples were collected on scans

from 5° to 50° two-theta at 1° degree stepwise per minute. PeakFit software (www.sigmaplot.com) was used to profile XRD patterns and evaluate the crystalline index.

2.4 Investigation of simulated *in-vitro* degradation of BC/CPs composites

BC/CPs composites (HASBFBC7, treated for 7 days) incorporating enzymes were placed in 10 mL of PBS, where a porous aluminum screen (24-mesh) capable of supporting samples on the interface between the medium and the air was used as described in our previous study to mimic the actual wound microenvironment.[29] The degradation progression was photographically recorded day by day until the samples were thoroughly degraded. Glucose released (GR) from the BC/CPs hydrogel composites on the last day examined was measured using the YSI 2700S Biochemistry Analyzer (YSI Inc., USA). The following equations were used to determine the percentage of actual glucose released to calculated glucose released, where 180 (g/mol) is the molecular weight of glucose and 162 (g/mol) is the molecular weight of an anhydroglucose unit losing one molecular H_2O.

$$\mathrm{GR} = \frac{\text{weight of dried BC sample without enzymes} \times 180}{162} \quad (1)$$

$$\mathrm{Ratio} = \frac{\text{actual GR}}{\text{calculated GR}} \times 100\% \quad (2)$$

2.5 Viability and morphology of mouse embryo preosteoblast cells on BC hydrogel composites

Mouse embryo preosteoblastic cells (MC3T3-E1, ATCC CRL2593) were activated and prepared following the method as described in the reference.[40] The complete culture medium for MC3T3-E1 consisted of α-MEM (Minimum Essential Media Alpha Modification, HyClone),

10% of FBS (Fetal Bovine Serum, Gibco) and 1% of Penicillin/Streptomycin (HyClone). BC samples containing pure BC, BC-HASBF and BC-1.5SBF were cut to an appropriate diameter of 10 mm and then placed into the 48-well non-treated culture plate. All the samples were immersed in 70% isopropanol for one hour, rinsed by PBS and then immersed in 0.5 mL of anhydrous ethanol overnight until the ethanol evaporated inside the clean hood. The cell suspension (approximately 100,000 cells/mL) of 0.5 mL was dropped onto the surface of each sample and MC3T3-E1 cells were seeded and grown at 37 °C for two days in an incubator with 5% CO_2.

For the observation of cell attachment and viability on BC samples using Laser Scanning Confocal Microscope (LSCM, Leica SD AF), samples were stained using the fluorescent dye fluorescein isothiocyanate (FITC). After two-day cultivation, the medium was carefully removed from culture plate and PBS was used to rinse the samples twice. Samples were subsequently fixed with 2.5% glutaraldehyde in PBS for 2 h at room temperature. FITC of 10 μg/mL was then used to dye the samples at 4 °C for 1 h after removing the fixing solution and washing samples with PBS. Samples after dehydration were observed under LSCM with an excitation wavelength of 488 nm.

For the observation of cell morphology on BC samples, cells attached on the samples on day 1 were fixed as described in our previous study.[41] After removing culture medium and rinsing the samples twice with PBS, 2.5% of glutaraldehyde was then applied to cover samples overnight at 4 °C. PBS was used again to rinse samples three times within 15-20 min. Next, a series of gradient concentrations of ethanol containing 25% ethanol (5 min), 50% ethanol (5 min), 70% ethanol (5 min), 85% ethanol (5 min), 95% ethanol (5 min), 100% ethanol (triple times, each for 5 min) was applied one by one to dehydrate samples. Subsequently, BC samples were soaked in

hexamethyldisilazane solution and placed in a biological hood until they were fully dehydrated. Dried samples were coated with gold and then observed by SEM operating at 5 kV.

2.6 Statistical analysis

All the experiments were repeated at least three times. The significant differences between sample groups were evaluated using One-Way ANOVA (LSD, Least Significant Difference) ($p < 0.05$ confident interval; IBM SPSS Statistical Software; Release 19.0.0).

3. Results and discussions

3.1 Material characterization of untreated BC, 1.5SBFBC and HASBFBC

SEM images in Fig. 1a-j show distinct surface morphologies of pure BC, 1.5SBFBC (7/14) and HASBFBC (7/14) specimens. The diameters of visible fibrous ribbons for different BC specimens were estimated in the range of 20-70 nm. As compared to pure BC, it was observed that a great number of apatite flakes aggregated and covered most fibrous ribbons of 1.5SBFBC7 as clearly shown in Fig. 3c. This was consistent with previous results using oversaturated SBF (1.5×) to grow apatite crystals.[12-17] Interestingly, in Fig. 1g and especially Fig. 1h showing higher magnifications, numerous globular aggregations in a size range of 40-300 nm were present surrounding the formed apatite flakes. Due to the presence of extra HA nanopowder and lower ionic concentration of SBF in the HASBFBC7 specimen, these small aggregations should be the deposition of CPs from HA nanopower dispersed in saturated SBF (1.0×). This suggests that the formation of apatite crystals might have contributed to the binding of more CPs to BC. Fig. 1e-f and 1i-j indicate the surface difference between immersing BC in oversaturated SBF and

saturated SBF with HA nanopowder when extending the processing time from 7 days to 14 days. The surface of HASBFBC7 (Fig. 1g) appeared to be much denser than 1.5SBFBC14 (Fig. 1e), although longer processing time (14 days) for samples in oversaturated SBF was used, suggesting that the presence of HA nanopowder in saturated SBF expedited the deposition of CPs on the BC. SEM observation verified the efficacy of using extra HA nanopowder dispersed in saturated SBF instead of exclusive oversaturated SBF to prepare BC composites, which bound more CPs to BC and reduced processing time.

Fig. 1. SEM images of: (a-b) pure BC; (c-f) 1.5SBFBC excluding HA nanopowder soaked in oversaturated SBF (1.5×) for 7 days and 14 days; (g-j) HASBFBC soaked in saturated SBF (1.0×) with additional HA nanopowder for 7 days and 14 days. Images b, d, f, h, j indicate higher magnifications as compared to images a, c, e, g, i, respectively.

The TGA thermograms of untreated BC, 1.5SBFBC and HASBFBC are shown in Fig. 2. Thermostability parameters including cellulose weight loss and decomposition temperature are summarized in Table 1. The percentage of weight loss between 150 **°C** to 450 **°C** is associated with the cellulose content in BC/CPs composites, while the weight loss after 400 **°C** may reflect the decomposition of mineral content which is not shown in our TGA thermograms.[11] The small peak around 40 **°C** is attributed to the weight loss of incorporated water adsorbed to BC or BC/CPs composites and is estimated to be approximately 5% from Fig. 2a. Since BC composites contain two distinct components (cellulose and minerals), we may estimate the content of minerals once the cellulose component in BC composites is determined. Table 1 shows no significant difference amongst data of weight losses for BC specimens prepared in either saturated SBF (1.0×) with additional HA nanopowder or oversaturated SBF (1.5×). DTG curves

as shown in Fig. 2b show the maximum decomposition temperature (T_{max}) and decomposition rate of cellulosic component at T_{max} in BC composites over a range of 350-400 °C.[42] The T_{max} and decomposition rate of BC/CPs composites remarkably declined as compared to untreated BC but no significant difference was found amongst all BC/CPs composites. However, the degrees of error in Table 1 show a certain difference that the weight loss associated with the cellulosic component of HASBFBC7/14 specimens appears to vary in a smaller range than 1.5SBFBC7/14 specimens, which suggests that the use of saturated SBF (1.0×) with additional HA nanopowder may result in a relatively more thermostable BC/CPs composites.

Fig. 2. TGA (a) and DTG (b) thermograms of untreated BC and BC/CPs composites prepared by soaking BC in oversaturated SBF (1.5×) and saturated SBF (1.0×) with additional HA nanopowder for 7 and 14 days.

Table 1. Weight loss and maximum decomposition temperature of the cellulosic component in BC/CPs composites.

The FTIR spectra of untreated BC, 1.5SBFBC and HASBFBC samples are illustrated in Fig. 3. Vertically numerical peaks on the untreated BC FTIR spectrum associated with 2895, 1336, 1315, 1162, 1109, 1057 and 1033 cm^{-1} are typical characters for cellulosic IR spectrum.[9] They disappear or decline in the absorbance intensity for other four samples of BC soaked in SBF with or without HA nanopowder, suggesting that BC fibers have been partly or fully covered by CPs. The bands between 3300 and 3400 cm^{-1} attribute to vibrations of intermolecular and intramolecular hydrogen bonding representing the hydroxyl groups of cellulose.[9] The reduction of OH^- ions for other treated BC soaked in SBF, as compared with untreated BC, may prove the

formation of CPs and the deposition of HA from SBF with additional HA nanopowder deposited on or around BC fibers. The absorbance intensity in this area for HASBFBC7/14 is much less than 1.5SBFBC7/14, suggesting that more CPs covering or being deposited on or around BC fibers for the case of BC soaked in SBF with additional HA nanopowder. The peaks at 748, 713, 666 cm^{-1} associated with the crystallinity of BC disappear or drop in the intensity for treated BC soaked in SBF as compared with untreated BC, which also suggests that BC/CPs composites may have a reduced crystallinity due to the formation or deposition of CPs around BC fibers.[16] Carboxyl groups (CO_3^{2-}) exhibited two absorbance peaks at 1423 and 873 cm^{-1}, representing the characteristic carbonate bands for the B-type HA (carbonate-substituted apatite) where the CO_3^{2-} group partially substitutes phosphate groups.[43] The formation of carbonate-substituted apatite may indicate more osseous bioactivity due to its composition and structure similar to natural bone.[44] The peaks at 1030 and 962 cm^{-1} only observed in spectra of treated BC soaked in SBF with and without HA are attributed to the stretching vibration of phosphate groups (PO_4^{3-}).[15] The PO_4^{3-} characteristic peaks are evidence of the formation and deposition of CPs on BC fibers. It should be noted that the FTIR spectra of HASBFBC7 and HASBFBC14 are quite similar to HA FTIR spectrum reported,[14,45] which may be evidence of almost full coverage of BC fibers by CPs for BC soaked in saturated SBF (1.0×) with additional HA nanopowder rather than BC only soaked in oversaturated SBF (1.5×). The FTIR analysis has demonstrated our hypothesis that the addition of HA nanopowder in saturated SBF could give rise to more CPs bound to BC as compared to oversaturated SBF used.

Fig. 3. FTIR spectra of untreated BC and BC/CPs composites prepared by soaking BC in oversaturated SBF (1.5×) and saturated SBF (1.0×) with additional HA nanopowder for 7 and 14 days.

The XRD patterns of BC, 1.5SBFBC and HASBFBC are shown in Fig. 4. The characteristic peaks at around 14.5°, 16.7°, 22.7° and 34.5° are associated with the cellulose component in the BC composites,[15] while those peaks at 25.8°, 27.3°, 31.7° and 45.4° are typically associated with CPs.[46] The decrease in the intensity of the XRD peaks associated with cellulose shown in Fig. 5, suggests that the presence of crystals of CPs have impacted cellulose crystallinity. This hypothesis is also based on the fact that the samples have very similar cellulose contents as shown in Table 1. Samples used for XRD analysis were also prepared to have the same size to avoid sample related artifacts. All peaks were fitted via PeakFit software where the peak at 21° was attributed to the amorphous content. The integral peak area was calculated for each peak and three ratios regarding the crystalline variation of composites were evaluated and summarized in Table 2. Ratio 1 represents the percentage variation of crystalline peak areas associated with the cellulosic component versus the crystalline peak areas associated with the formed CPs. Ratio 2 represents the percentage variation of crystalline peak areas of the cellulosic component in BC/CPs composites. Ratio 3 is the crystallinity of the cellulosic component in BC/CPs composites calculated by ignoring the mineral peaks. As shown in Table 2, the ratio of crystalline area of the cellulosic component declined as the amount of formed CPs increased. This ratio dramatically decreased in BC/CPs composites as compared to the pure BC. It has been shown that the deposition of CPs on the surface would lead to the formation of certain crystals with low crystallinity.[14] The reduced crystalline ratio involving the cellulosic component in different BC/CPs composites was due to the formation of CPs. By using saturated SBF (1.0×) with

additional HA nanopowder, the ratio of crystalline peak areas of the cellulosic component decreased more significantly than in the case where oversaturated SBF (1.5×) was used. The short-term treatment (7 days) using saturated SBF (1.0×) with additional HA nanopowder achieved a lower ratio of crystalline areas associated with the cellulose component (1.07±0.017) than the long-term treatment (14 days) using oversaturated SBF (1.5×) (1.66±0.012). Ratio 3 in Table 2 revealed that the crystallinity of the cellulosic component in BC/CPs composites prepared in the oversaturated SBF (1.5×) was indeed decreased as compared to pure BC, while this influence on BC/CPs composites prepared in the saturated SBF (1.0×) with additional HA nanopowder did not impact the crystallinity of the cellulosic component. Owing to the unobvious variation of crystallinity as compared to pure BC, BC/CPs composites may be relatively more thermostable if prepared in the saturated SBF with addition HA nanopowder than oversaturated SBF. XRD analyses suggest that the dual influence from biomineralization of SBF and deposition of HA nanopowder in saturated SBF (1.0×) with additional HA nanopowder may expedite the formation of more CPs on the surface of BC, resulting in more thermostable composites.

Fig. 4. XRD patterns of untreated BC and BC/CPs composites prepared by soaking BC in oversaturated SBF (1.5×) and saturated SBF (1.0×) with additional HA nanopowder for 7 and 14 days.

Table 2. Crystallinity analysis results of untreated BC and BC/CPs composites prepared by soaking BC in oversaturated SBF (1.5×) and saturated SBF (1.0×) with additional HA nanopowder for 7 and 14 days.

Research has elucidated that the formation of apatite layers is strongly subject to ionic strength.[16] It has been documented that amine groups, silanol groups, hydroxyl groups, carboxyl groups, phosphate groups, sodium silicate gel layers, and even calcium salts can initiate apatite formation.[16,47-48] The oversaturated SBF (1.5×) is broadly used to grow bioactive apatite layers on biomaterials, while no explicit reason was given in the reference to explain why oversaturated SBF (1.5× or higher concentrations) is often used rather than saturated SBF (1.0×). One possibility is that the use of oversaturated SBF is due to the oversaturated ion concentration that can trigger the formation calcium nucleus clusters to induce the formation of apatite layers.[49-51] In this study, we believe that the deposition of more CPs on BC using saturated SBF with additional HA nanopowder as compared to oversaturated SBF could be hypothetically explained in Fig. 5. The first phase describes the formation of apatite crystal layers by the aggregation of HA nuclei initiated by hydroxyl-calcium ionic-dipolar interaction, which has been demonstrated.[13,16] The second phase might involve a common ion effect,[52] where the partly dissolved HA may release phosphate groups to result in more CPs salting out from the SBF solution to increase the aggregation of apatite compounds. The last phase is related to the homogeneous ion adsorption that probably occurs between HA and newly formed apatite crystals or active calcium-ion layers.[53,54] It is noticed that common ion effect and homogeneous ion adsorption are weak due to the lack of HA nanopowder in oversaturated SBF, which leads to less deposition of CPs as compared to saturated SBF with the additional HA nanopowder. The above analyses from SEM, TGA, FTIR and XRD have further verified our hypothesis that the improved approach of using saturated SBF with HA nanopowder to prepare BC/CPs composites could make CPs more likely to deposit on BC.

Fig. 5. Schematic illustration of the mechanism of apatite crystal formation and CPs bound to BC in saturated SBF (1.0×) containing additional HA nanopowder.

3.2 *In vitro* degradation

Fig. 6g-l shows the degradation progression of BC/CPs composite (HASBFBC7) containing cellulosic enzyme over five days as compared to the pure BC containing same enzyme (Fig. 6a-f). It was observed that BC/CPs composite in the presence of cellulosic enzyme could completely degrade, but CPs bound to BC appeared to slow down the degradation rate of BC/CPs composite. This should be due to the density increase of BC/CPs composite that reduced the accessible cellulose surface area that cellulosic enzyme could reach. Additionally, Fig. 6 reveals that either pure BC or BC/CPs composite exhibited a bulk degradation behavior rather than a block-by-block collapse. The "block-by-block" degradation behavior begins with an initial decomposition of the material into some small fragments that would continuously decrease in size until they are no longer visible. In this case, the material quickly loses its ability to provide adequate mechanical support for cells to attach and proliferate. Meanwhile, those small fragments can easily give rise to the thrombus or clogging which may retard tissue regeneration or more severely cause a tumor.[55] However, the bulk degradation of the material does not collapse into small fragments, and it would rather reduce in volume or density until it is no longer visible. It is a better degradation behavior especially for those wounds that need materials to fill as well as provide a persistent mechanical support. In Fig. 6, the BC incorporating enzyme exhibited such a bulk degradation behavior rather than block-by-block degradation, which would be more appropriate for bone defect filling to prevent the remain of material debris from forming thrombus or local tumors.[56,57]

The yields of glucose from the degradation of BC and BC/CPs composite were calculated as 98% for pure BC and 96% for BC/CPs composite. No significant difference ($p<0.05$) of glucose yields for both samples was present. As mentioned above, the oxidized cellulose could achieve biodegradation by physiologically chemical erosion *in-vitro* and *in-vivo*.[58] However, no evidence was shown that the major degradation products were monosaccharides. It is believed that the chemical degradation of cellulose mostly results in more oligocelluloses, while the enzymatic degradation of cellulose is able to finally obtain glucose.[27,28] Given that glucose can be used as a nutrient for cell growth, the enzymatic degradation is considered a more ideal approach for accomplishing a complete bioabsorption of cellulose in the body.

Fig. 6. Photographs depicting the degradation processes of (a)-(f) pure BC incorporating cellulosic enzyme and (g)-(l) BC/CPs composite (HASBFBC7) incorporating cellulosic enzyme over 5 days.

3.3 Cell culture and cell morphology

The attachment and proliferation in the two-day cultivation of MC3T3-E1 on pure BC, 1.5SBFBC7/14 and HASBFBC7/14 were analyzed as shown in Fig. 7a-e. The attachment of MC3T3-E1 showed significant differences between 1.5SBFBC and HASBFBC specimens. A preferable viability of MC3T3-E1 cells was found in HASBFBC specimens (Fig. 7d-e) as compared to 1.5SBFBC specimens (Fig. 7b-c). We hypothesize that this may be due to the increased surface density of HASBFBC as compared to 1.5SBFBC specimens, suggesting that a denser surface covered by more CPs may facilitate cells to grow. The cell morphology of MC3T3-E1 cells on BC and BC composites was observed under SEM as shown in Fig. 7a-e.

MC3T3-E1 cells were able to attach and spread well on almost all the BC specimens containing pure BC, 1.5SBFBC and HASBFBC. However, a careful observation has given the fact that MC3T3-E1 cells achieved a better scattering attachment on HASBFBC specimens (Fig. 8d-e) as compared to pure BC and 1.5SBFBC specimens. This could also be due to the formation of a flatter or denser surface area in HASBFBC specimens where more CPs bound to BC led to a different surface structure, such as porosity or stiffness, to improve the cell attachment. The HASBFBC specimens offered MC3T3-E1 cells better viability and morphology than pure BC and 1.5SBFBC over the culturing period, suggesting that the formation and deposition of more CPs onto BC would greatly improve biocompatible behavior of BC. As a result, we believed that this unique BC/CPs composite prepared by soaking BC in saturated SBF with additional HA nanopowder instead of oversaturated SBF would benefit the physiological activities of cells, as well as, provide a temporary substrate for cell growth. If incorporating enzyme to the BC composite, its bioabsorption would be readily achieved.

Fig. 7. Cell viability of MC3T3-E1 cells after two-day culture on: (a) the pure BC; (b-c) BC/CPs composite prepared by soaking BC in oversaturated SBF (1.5×) for 7 and 14 days; (d-e) BC/CPs composite prepared by soaking BC in saturated SBF (1.0×) with additional HA nanopowder for 7 and 14 days.

Fig. 8. Cell morphology of MC3T3-E1 cells after a two-day cultivation on: (a) the pure BC; (b-c) BC/CPs composite prepared by soaking BC in oversaturated SBF (1.5×) for 7 and 14 days; (d-e) BC/CPs composite prepared by soaking BC in saturated SBF (1.0×) with additional HA nanopowder for 7 and 14 days.

4. Conclusions

This work used an improved approach to prepare a bioabsorbable BC composite that could achieve more bio-CPs formed or deposited on BC in saturated SBF (1.0×) with additional HA nanopowder than oversaturated SBF (1.5×). SEM, TGA, FTIR, and XRD analyses have given evidences of more CP molecules bound to the BC fibrous network, as well as, more hydrate HA compounds formed in BC/CPs composites prepared by such an improved approach. Upon the incorporation of cellulosic enzyme into BC composite, the nearly complete *in-vitro* bioabsorption of BC composite was achieved, suggesting its potential to act as a biodegradable carrier to deliver CPs to bone defect sites. Additionally, cell viability study of MC3T3-E1 demonstrated that such a bioabsorbable BC composite prepared by soaking BC in saturated SBF (1.0×) with additional HA nanopowder exhibited a better biocompatibility than using oversaturated SBF (1.5×), which further suggests that it could function not only as a temporary carrier delivering CPs as many as possible but also as a good temporary substrate providing mechanical and nutrient supports for cell growth.

Acknowledgement

This work was supported by the National Natural Science Foundation of China no. 31570967; the Guangdong Natural Science Foundation no.S2013040014248; the Shenzhen Science and Technology Program no.JCYJ20140610152828698; the Shenzhen Peacock program

no. 110811003586331; the Shenzhen Key Laboratory of Marine Biomedical Materials no. ZDSY20130401165820356.

References

1. J. Aerssens, S. Boonen, G. Lowet and J. Dequeker, *Endocrinology*, 1998, 139, 663-670.
2. P. P. Spicer, J. D. Kretlow, S. Young, J. A. Jansen, K. F. Kasper and A. G. Mikos, *Nat. Protoc.*, 2012, 7, 1918-1929.
3. S. Zwingenberger, E. Niederlohmann, C. Vater, S. Rammelt, R. Matthys, R. Bernhardt, R. D. Valladares, S. B. Goodman and M. Stiehler, *J. Surg. Res.*, 2013, 181, e7-e14.
4. I. Siró and D. Plackett, *Cellulose*, 2010, 17, 459-494.
5. A. N. Nakagaito, S. Iwamoto and H. Yano, *Appl. Phys. A*, 2005, 80, 93-97.
6. W. K. Czaja, D. J. Young, M. Kawechi and R. M. Brown, *Biomacromolecules*, 2007, 8, 1-12.
7. Y. Hu, J. M. Catchmark, Y. J. Zhu, N. Abidi, X. Zhou, J. H. Wang and N. Y. Liang, *J. Mater. Res.*, 2014, 29, 2682-2693.
8. J. Andersson, H. Stenhamre, H. Bäckdahl and P. Gatenholm, *J. Biomed. Mater. Res. A*, 2010, 94A, 1124-1132.
9. L. Hong, Y. L. Wang, S. R. Jia, Y. Huang, C. Gao and Y. Z. Wan, *Mater. Lett.*, 2006, 60, 1710-1713.

10. A. Svensson, E. Nicklasson, T. Harrah, B. Panilaitis, D. L. Kaplan, M. Brittberg and P. Gatenholm, *Biomaterials*, 2006, 26, 419-431.

11. C. J. Grande, F. G. Torres, C. M. Gomez and M. Bañó, *Acta Biomater.*, 2009, 5, 1605-1615.

12. B. Fang, Z. Y. Wan, T. T. Tang, C. Gao and K. R. Dai, *Tissue Eng. Pt. A*, 2009, 15, 1091-1098.

13. S. A. Hutchens, R. S. Benson, B. R. Evans, H. M. O'Neill and C. J. Rawn, *Biomaterials*, 2006, 27, 4661-4670.

14. S. Shi, S. Chen, X. Zhang, W. Shen, X. Li, W. Hu and H. Wang, *J. Chem. Technol. Biotechnol.*, 2009, 84, 285-290.

15. Y. Z. Wan, L. Hong, S. R. Jia, Y. Huang, Y. Zhu, Y. L. Wang and H. J. Jiang, *Compos. Sci. Technol.*, 2006, 66, 1825-1832.

16. Y. Z. Wan, Y. Huang, C. D. Yuan, S. Raman, Y. Zhu, H. J. Jiang, F. He and C. Gao, *Mat. Sci. Eng. C-Mater.*, 2007, 27, 855-864.

17. K. A. Zimmermann, J. M. LeBlanc, K. T. Sheets, R. W. Fox and P. Gatenholm, *Mat. Sci. Eng. C Mater.*, 2011, 31, 43-49.

18. G. Helenius, H. Bäckdahl, A. Bodin, U. Nannmark, P. Gatenholm and B. Risberg, *J. Biomed. Mater. Res. A*, 2006, 76, 431-438.

19. C. Ruan, N. Hu, Y. Hu, L. Jiang, Q. Cai, H. Wang, H. Pan, W. W. Lu and Y. Wang, *Polymer*, 2014, 55, 1020-1027.

20. C. Ruan, Y. Hu, L. Jiang, Q. Cai, H. Pan and H. Wang, *J. Appl. Polym. Sci.*, 2014, 131, 40527-40532.

21. L. J. Christenson, C. C. Otley and R. K. Roenigk, *Dermatol. Surg.*, 2004, 30, 1593-1594.

22. M. Merle, B. Lallemand and A. Lim, *Eur. J. Orthop. Surg. Traumatol.*, 2008, 18, 255-263.

23. S. D. Dimitrijevich, M. Tatarko and R. W. Gracy, *Carbohyd. Res.*, 1990, 195, 247-256.

24. J. Li, Y. Z. Wan, L. F. Li, H. Liang and J. H. Wang, *Mat. Sci. Eng. C-Mater.*, 2009, 29, 1635-1642.

25. S. Reddy, N. Santanam, P. P. Reddy, J. A. Rock, A. A. Murphy and S. Parthasarathy, *Am. J. Obstet. Gynecol.*, 1997, 177, 1315-1321.

26. K. Sutherland, J. R. Mahoney, A. J. Coury and J. W. Eaton, *J. Clin. Invest.*, 1993, 92, 2360–2367.

27. M. J. Taherzadeh and K. Karimi, *BioResources*, 2007, 2, 472-499.

28. M. J. Taherzadeh and K. Karimi, *BioResources*, 2007, 2, 707-738.

29. Y. Hu and J. M. Catchmark, *Acta. Biomater.*, 2011, 7, 2835-2845.

30. Y. Hu and J. M. Catchmark, *J. Biomed. Mater. Res. B*, 2011, 97B, 114-123.

31. J. M. Catchmark, B. Fugmann and Y. Hu, *Degradable biomolecule compositions*, United States Patent Application 20100172889.

32. M. Bohner and J. Lemaitre, *Biomaterials*, 2009, 30, 2175-2179.

33. T. Kokubo and H. Takadama, *Biomaterials*, 2006, 27, 2907-2915.

34. Y. Hu and J. M. Catchmark, *Biomacromolecules*, 2010, 11, 1727-1734.

35. Y. Hu and J. M. Catchmark, *Lett. Appl. Microbiol.*, 2010, 51, 109-113.

36. T. Kokubo, H. Kushitani, S. Sakka, T. Kitsugi and T. Yamamuro, *J. Biomed. Mater. Res.*, 1990, 24, 721-734.

37. T. Kokubo, S. Ito, Z. T. Huang, T. Hayashi, S. Sakka, T. Kitsugi and T. Yamamuro, *J. Biomed. Mater. Res.*, 1990, 24, 331-343.

38. J. Ni and M. Wang, *Mat. Sci. Eng. C-Mater.*, 2002, 20, 101-109.

39. J. Gu and J. M. Catchmark, *Carbohyd. Polym.*, 2012, 88, 547-557.

40. R. F. Brown, M. N. Rahaman, A. B. Dwilewicz, W. Huang, D. E. Day, Y. Li and B. S Bal, *J. Biomed. Mater. Res. A*, 2008, 88A, 392-400.

41. Y. Hu, J. M. Catchmark and E. A. Vogler, *Biomacromolecules*, 2013, 14, 3444-3452.

42. S. Zhang, G. Xiong, F. He, Y. Huang, Y. Wang and Y. Wan, *Polym. Composite.*, 2009, 17, 353-358.

43. L. F. Sukhodub, C. Moseke, L. B. Sukhodub, B. Sulkio-Cleff, V. Y. Maleev, M. A. Semenov, E. G. Bereznyak and T. V. Bolbukh, *J. Mol. Struct.*, 2004, 704, 53-58.

44. P. Li, C. Ohtsuki, T. Kokubo, K. Nakanishi, N. Soga and K. de Groot, *J. Biomed. Mater. Res.*, 1994, 28, 7-15.

45. A. C. Tas, *Biomaterials*, 2000, 21, 1429-1438.

516 46. L. Cao, C. Zhang and J. Huang, *Mater. Lett.*, 2005, 59, 1902-1906.

517 47. P. L. Granja, C. C. Ribeiro, B. De Jéso, C. Baquey and M. A. Barbosa, *J. Mater. Sci. Mater.*
518 *Med.*, 2001, 12, 785-791.

519 48. A. L. Oliveira, P. B. Malafaya and R. L. Reis, *Biomaterials*, 2003, 24, 2575-2584.

520 49. S. H. Rhee and J. Tanaka, *J. Mater. Sci. Mater. Med.*, 2000, 11, 449-452.

521 50. J. Xin, T. Chen, Z. Lin, P. Dong, H. Tan and J. Li, *Chem. Commun.*, 2014, 6491-6493.

522 51. Z. Lin, S. Cao, X. Chen, W. Wu and J. Li, *Biomacromolecules*, 2013, 14, 2206-2214.

523 52. E. Fernández, M. G. Boltong, M. P. Ginebra, O. Bermúdez, F. C. M. Driessens and J. A.
524 Planell, *Clin. Mater.*, 1994, 16, 99-103.

525 53. T. Gotoh, K. Matsushima and K. I. Kikuchi, *Chemosphere*, 2004, 55, 135-140.

526 54. M. Ogawa and H. Kaiho, *Langmuir*, 2002, 18, 4240-4242.

527 55. W. Friess, *Eur. J. Pharm. Biopharm.*, 1998, 45, 113-136.

528 56. D. F. Williams, *Biomaterials*, 2008, 29, 2941-2953.

529 57. L. Yang and T. J. Webster, *Biological responses to and toxicity of nanoscale implant*
530 *materials. In Degradation of Implant Materials*, Noam E, 2012, p. 481-507.

531 58. W. Czaja, D. Kyryliouk, C. A. DePaula and D. D. Buechter, *J. Appl. Polym. Sci.*, 2014, 131,
532 39995-40006.

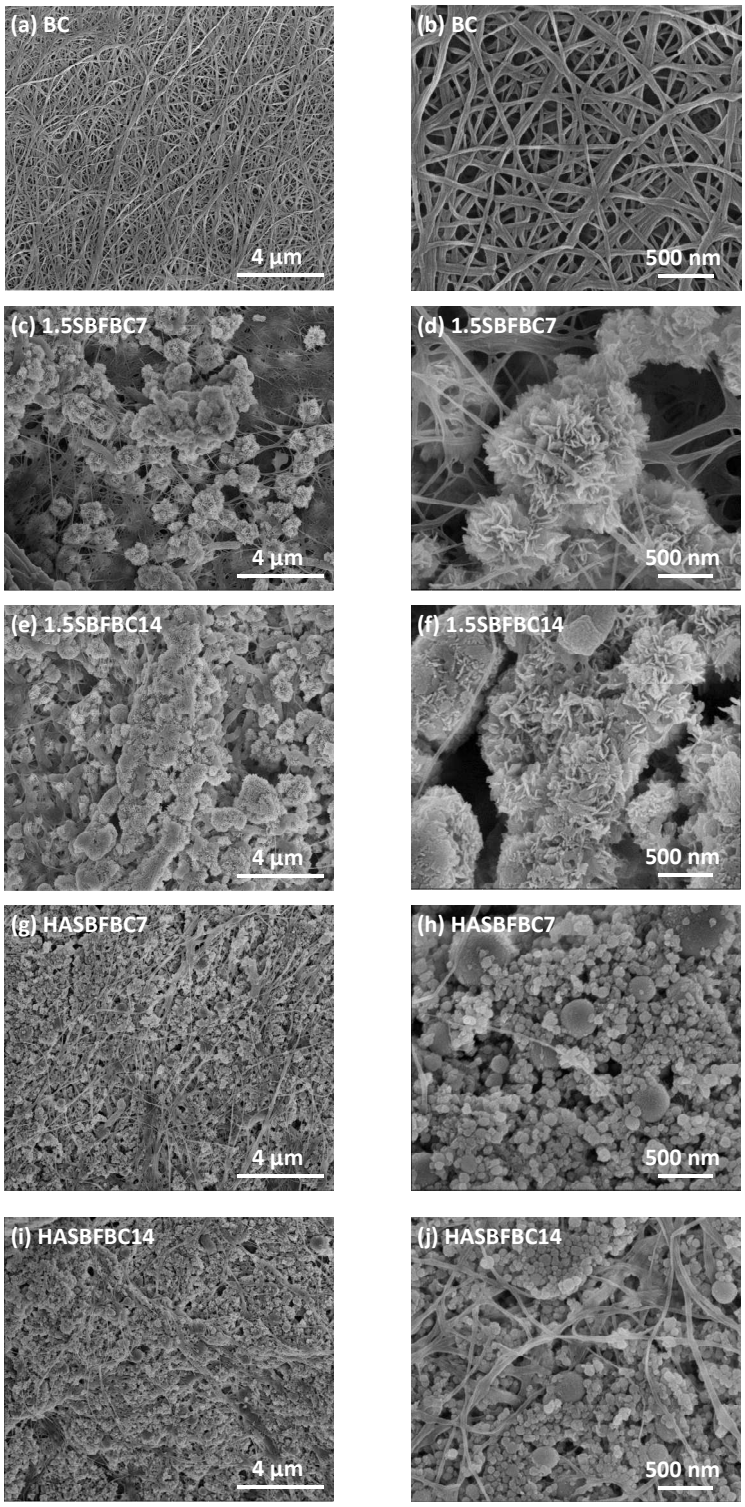

Fig. 1. SEM images of: (a-b) pure BC; (c-f) 1.5SBFBC excluding HA nanopowder soaked in oversaturated SBF (1.5×) for 7 days and 14 days; (g-j) HASBFBC soaked in saturated SBF (1.0×) with additional HA nanopowder for 7 days and 14 days. Images b, d, f, h, j indicate higher magnifications as compared to images a, c, e, g, i, respectively.

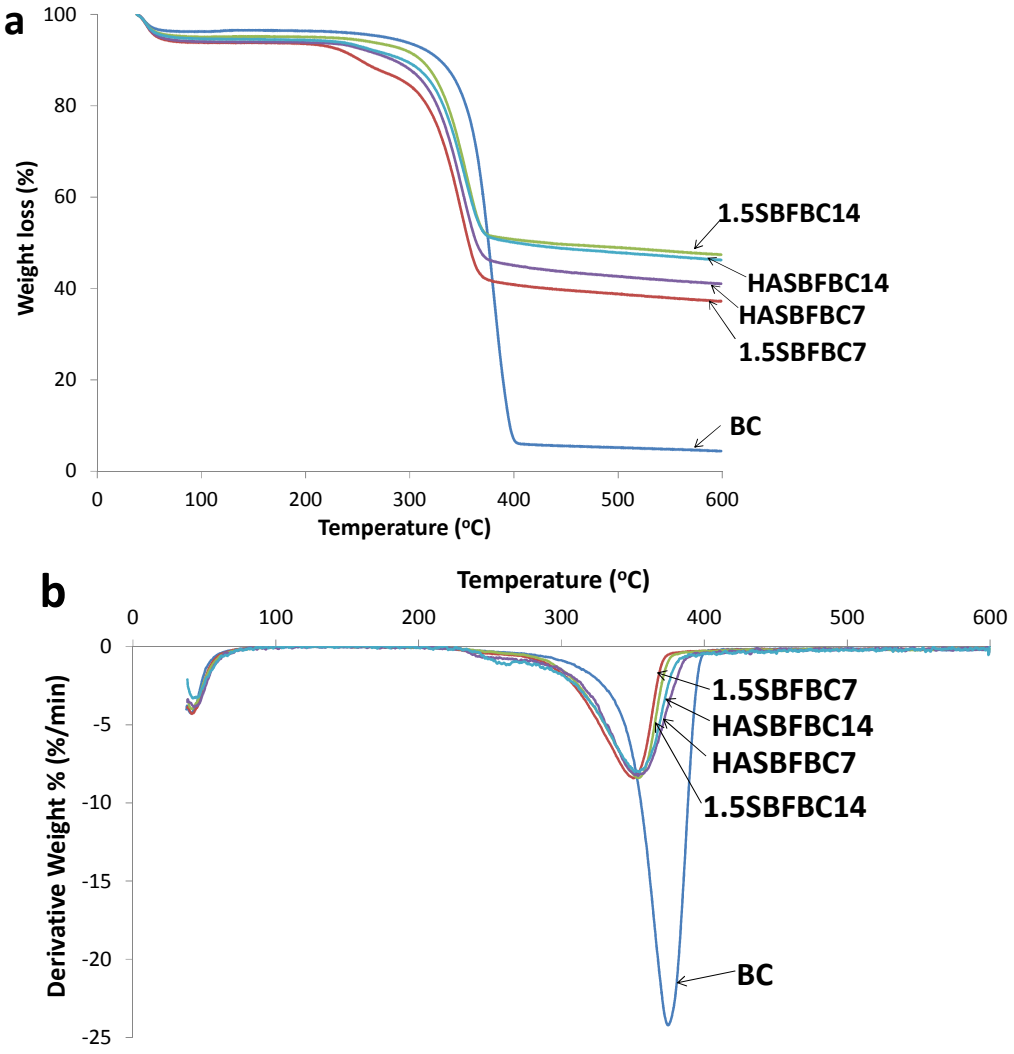

Fig. 2. TGA (a) and DTG (b) thermograms of untreated BC and BC/CPs composites prepared by soaking BC in oversaturated SBF (1.5×) and saturated SBF (1.0×) with additional HA nanopowder for 7 and 14 days.

Table 1. Weight loss and maximum decomposition temperature of the cellulosic component in BC/CPs composites.

Samples ID	Weight loss (%)*	T_{max} (°C) at decomposition**
BC	90.37±2.59	375.9±3.2
1.5SBFBC7	48.70±6.80	350.4±0.4
1.5SBFBC14	44.59±3.45	354.7±1.2
HASBFBC7	51.68±2.06	351.4±2.5
HASBFBC14	45.37±0.95	354.3±1.3

*The percentage of weight loss of cellulose in BC and BC composites is calculated between 150 and 450 °C.
**T_{max} is the maximum decomposition temperature of BC and BC composites calculated from DTG curve.

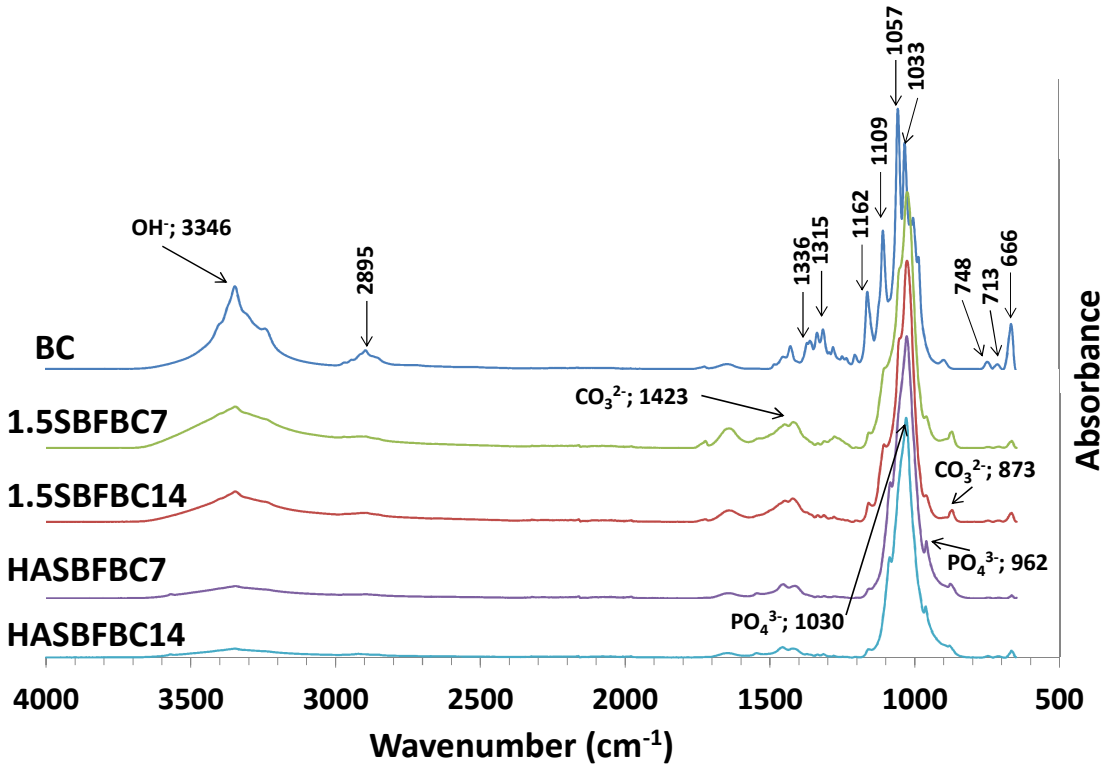

Fig. 3. FTIR spectra of untreated BC and BC/CPs composites prepared by soaking BC in oversaturated SBF (1.5×) and saturated SBF (1.0×) with additional HA nanopowder for 7 and 14 days.

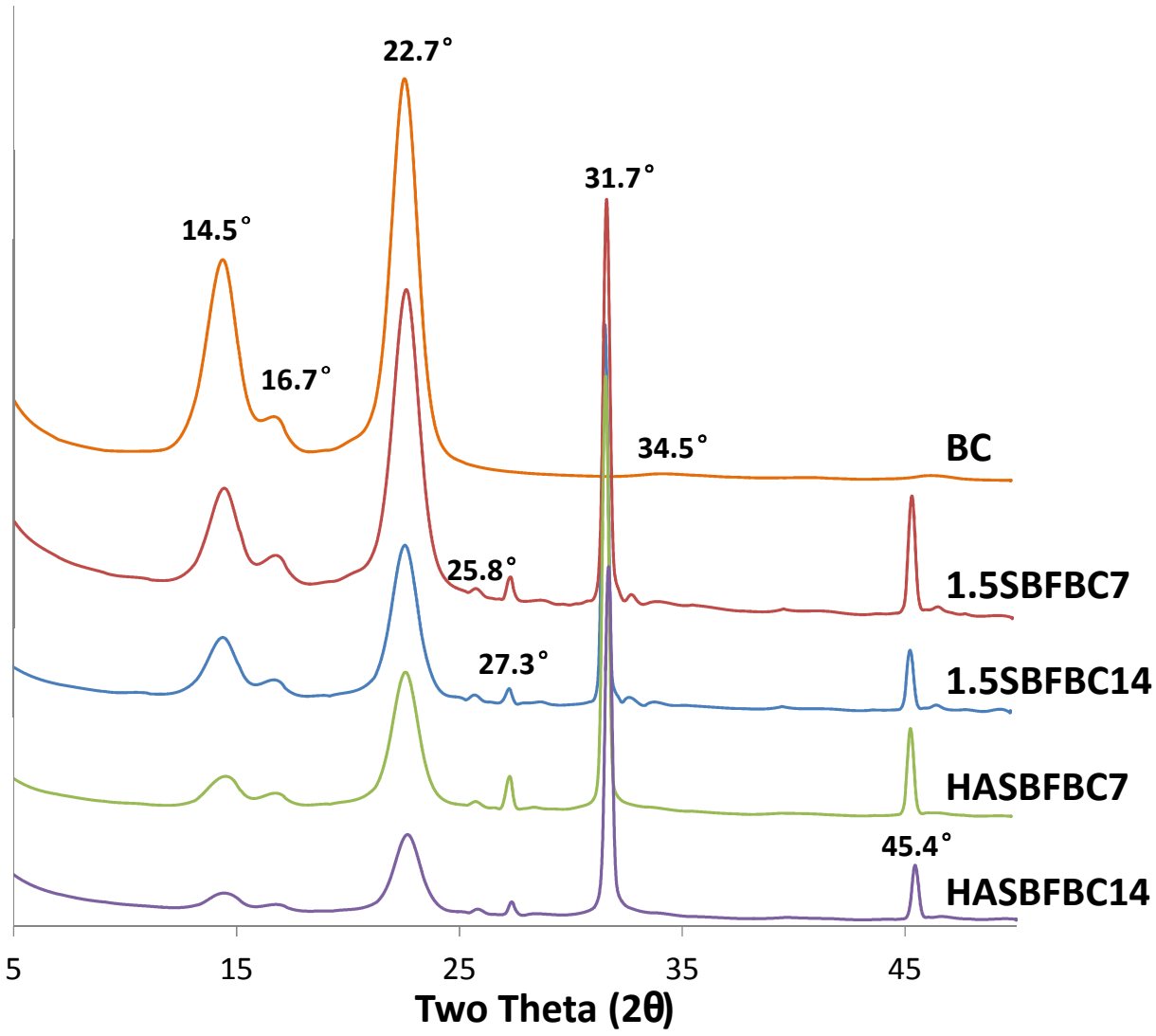

Fig. 4. XRD patterns of untreated BC and BC/CPs composites prepared by soaking BC in oversaturated SBF (1.5×) and saturated SBF (1.0×) with additional HA nanopowder for 7 and 14 days.

Table 2. Crystallinity analysis results of untreated BC and BC/CPs composites prepared by soaking BC in oversaturated SBF (1.5×) and saturated SBF (1.0×) with additional HA nanopowder for 7 and 14 days.

BC specimens / **XRD Analysis**	**BC**	**1.5SBFBC7**	**1.5SBFBC14**	**HASBFBC7**	**HASBFBC14**
Ratio 1 *	N/A	2.33±0.165	1.66±0.012	1.07±0.017	0.74±0.027
Ratio 2 *	0.86±0.01	0.60±0.015	0.52±0.011	0.47±0.015	0.39±0.013
Ratio 3 **	86±1%	81±1%	75±2%	83±4%	82±3%

* $Ratio\,1 = \frac{\Sigma(BC\ crystalline\ peak\ areas)}{\Sigma(CPs\ crystalline\ peak\ areas)}$, $Ratio\,2 = \frac{\Sigma(BC\ crystalline\ peak\ areas)}{\Sigma(all\ peak\ areas)}$.

** Crystallinity of BC in BC/CPs composites: $Ratio\,3 = \frac{\Sigma(BC\ crystalline\ peak\ areas)}{\Sigma(BC\ crystalline\ and\ amorphous\ peak\ areas)} \times 100$

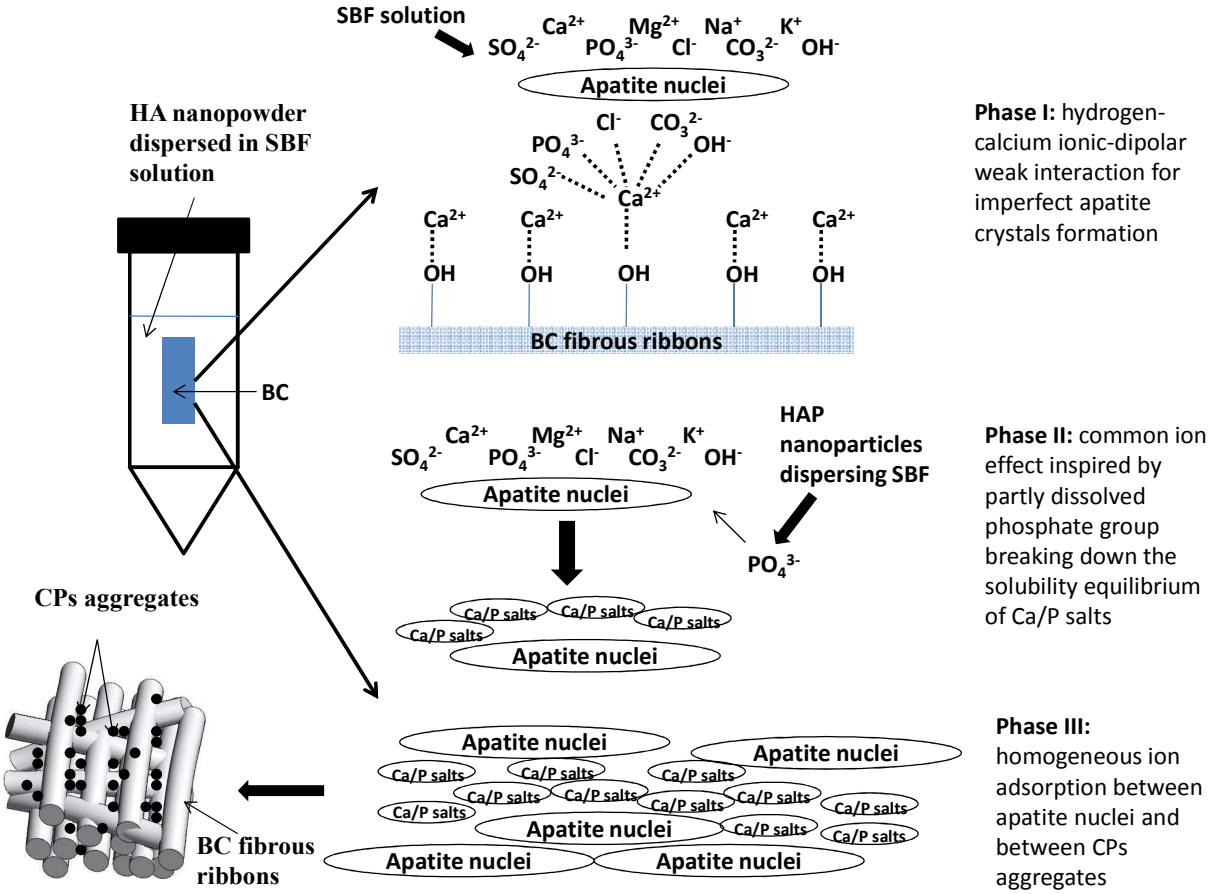

Fig. 5. Schematic illustration of the mechanism of apatite crystal formation and CPs bound to BC in saturated SBF (1.0×) containing additional HA nanopowder.

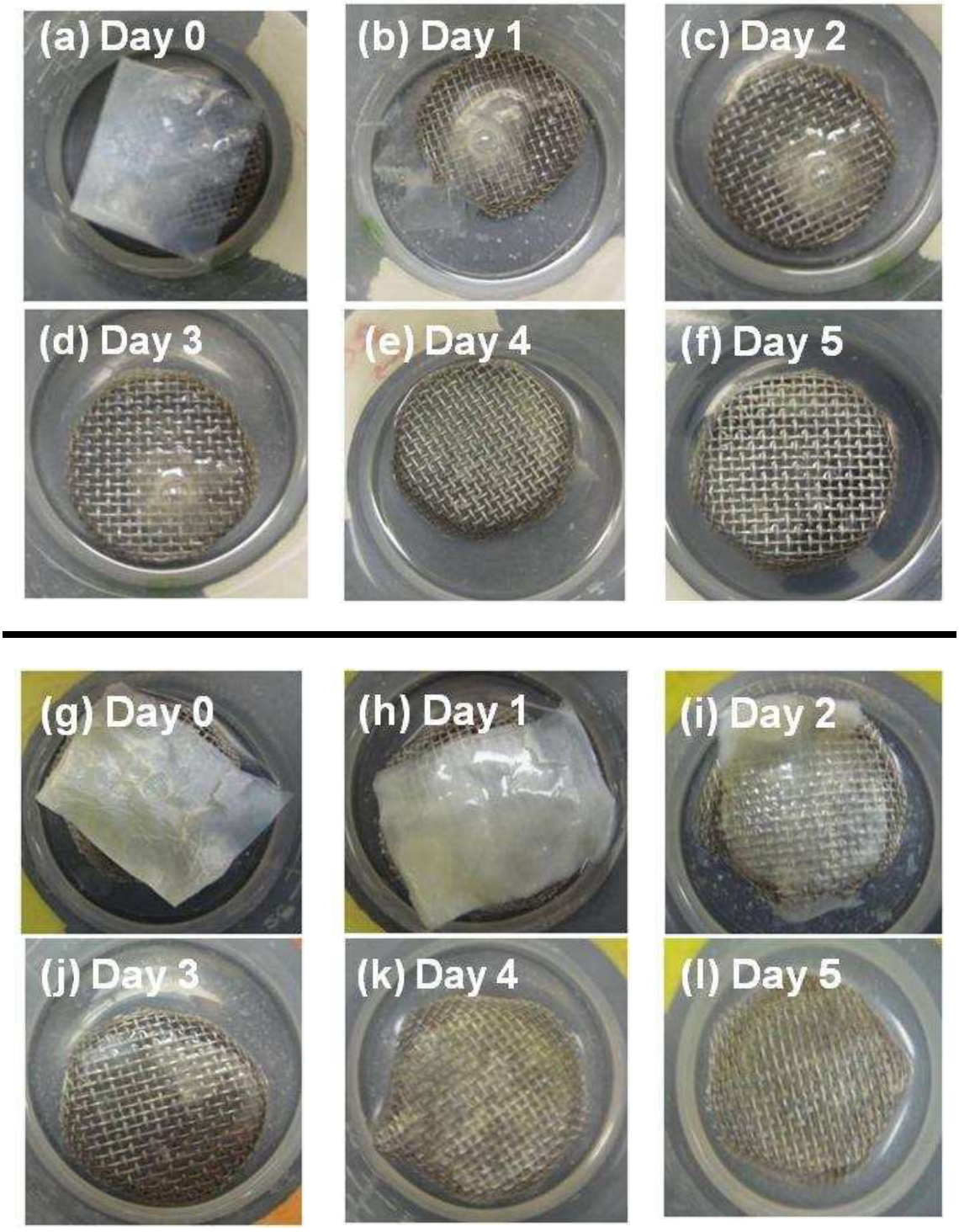

Fig. 6. Photographs depicting the degradation processes of (a)-(f) pure BC incorporating cellulosic enzyme and (g)-(l) BC/CPs composite (HASBFBC7) incorporating cellulosic enzyme over 5 days.

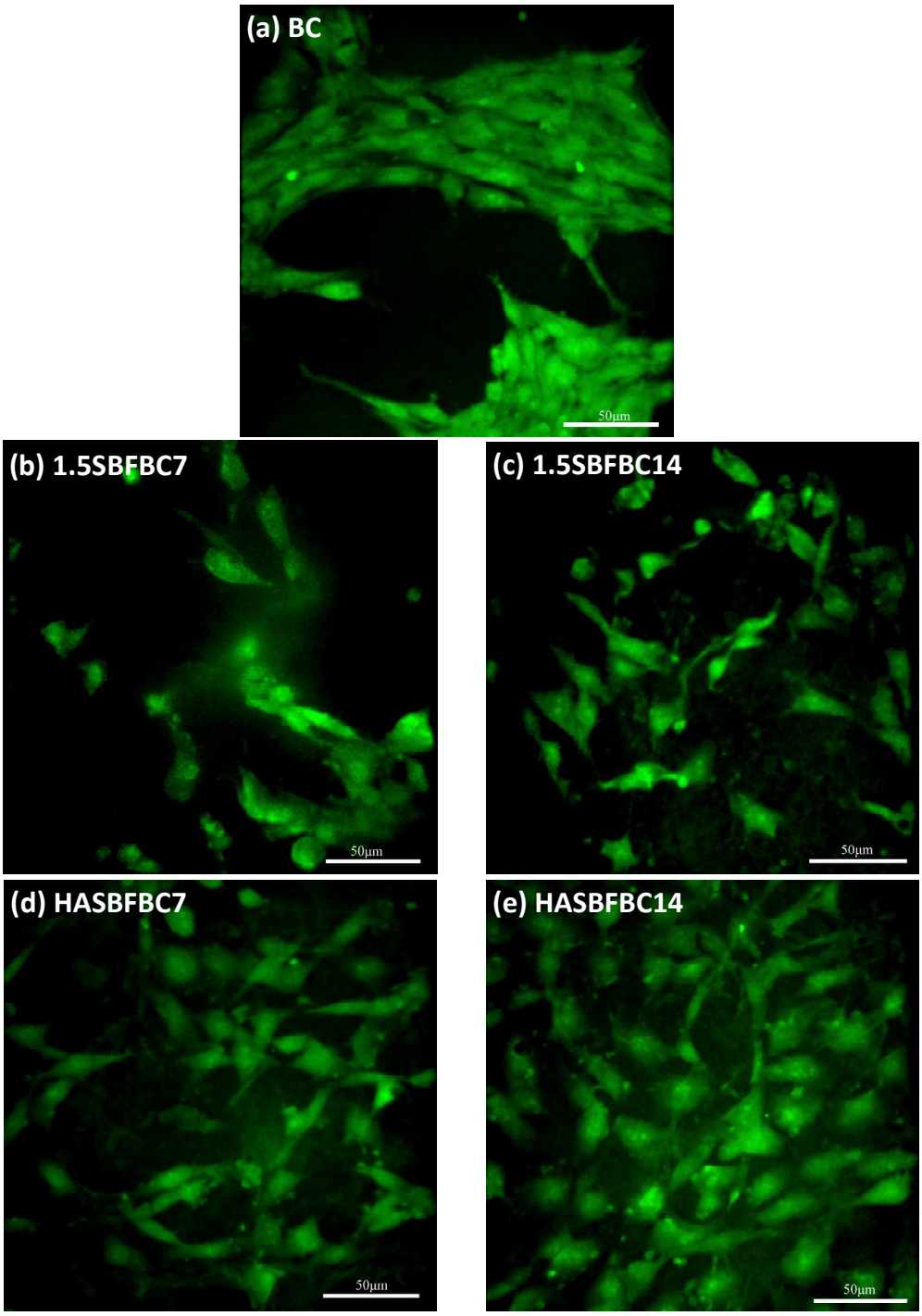

Fig. 7. Cell viability of MC3T3-E1 cells after two-day culture on: (a) the pure BC; (b-c) BC/CPs composite prepared by soaking BC in oversaturated SBF (1.5×) for 7 and 14 days; (d-e) BC/CPs composite prepared by soaking BC in saturated SBF (1.0×) with additional HA nanopowder for 7 and 14 days.

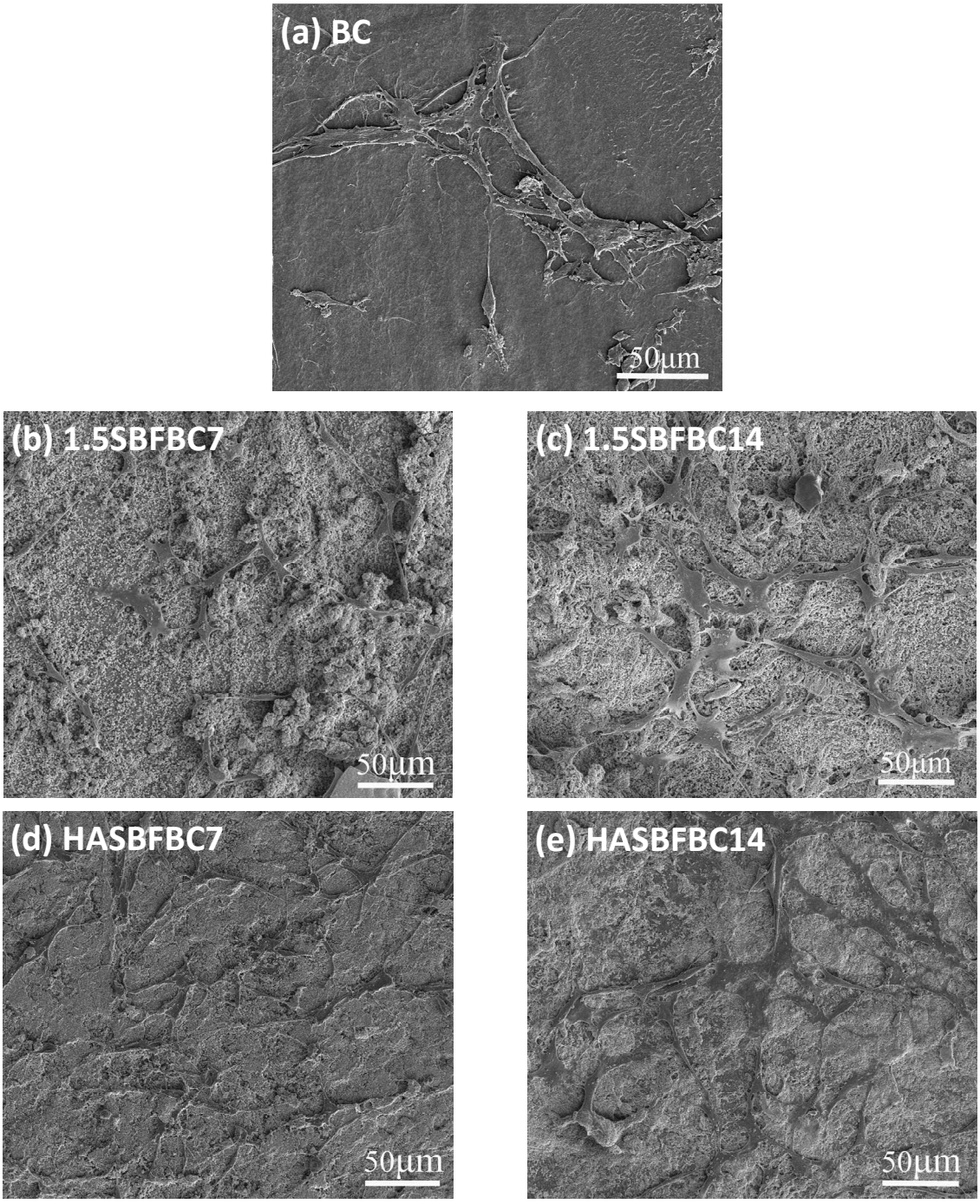

Fig. 8. Cell morphology of MC3T3-E1 cells after a two-day cultivation on: (a) the pure BC; (b-c) BC/CPs composite prepared by soaking BC in oversaturated SBF (1.5×) for 7 and 14 days; (d-e) BC/CPs composite prepared by soaking BC in saturated SBF (1.0×) with additional HA nanopowder for 7 and 14 days.

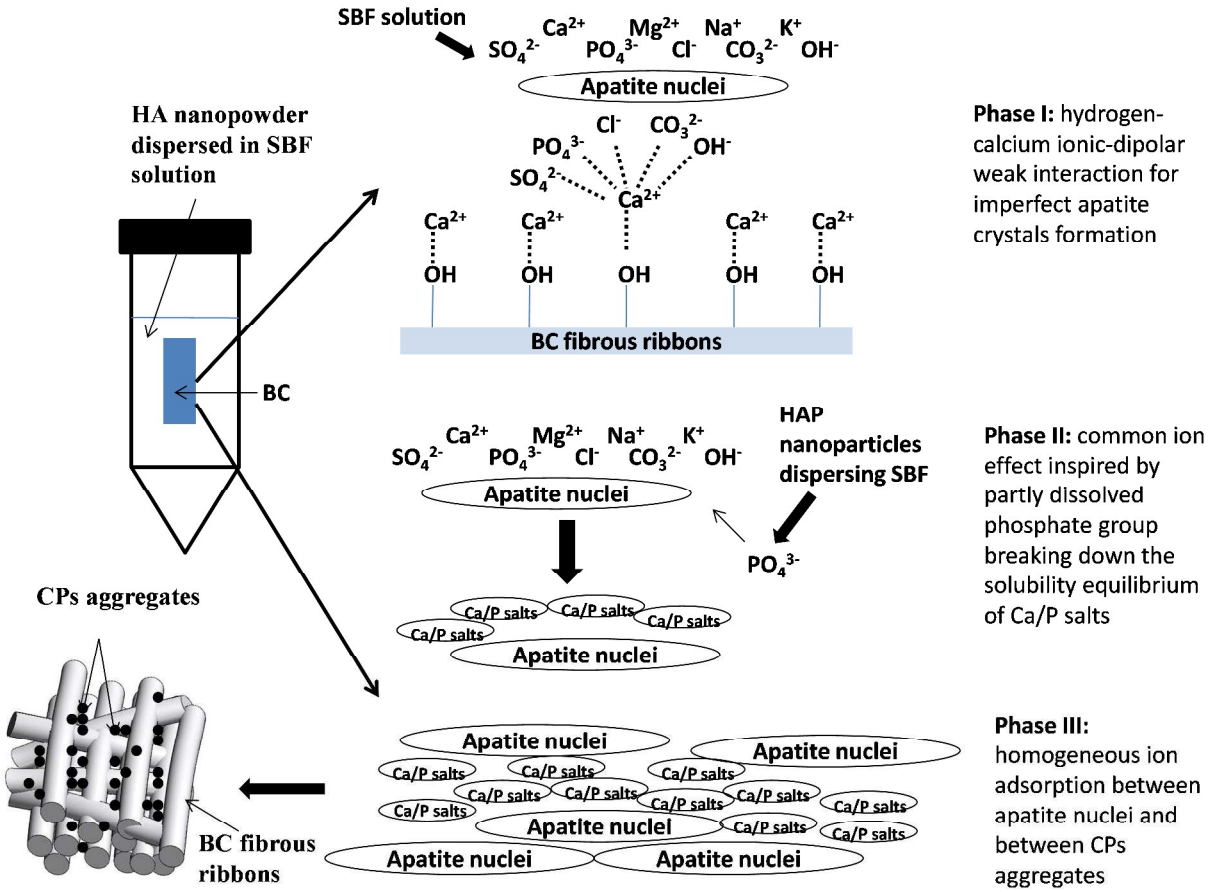

An improved mineral-binding approach was used to expedite the deposition of CPs on BC materials in HA contained SBF solution.